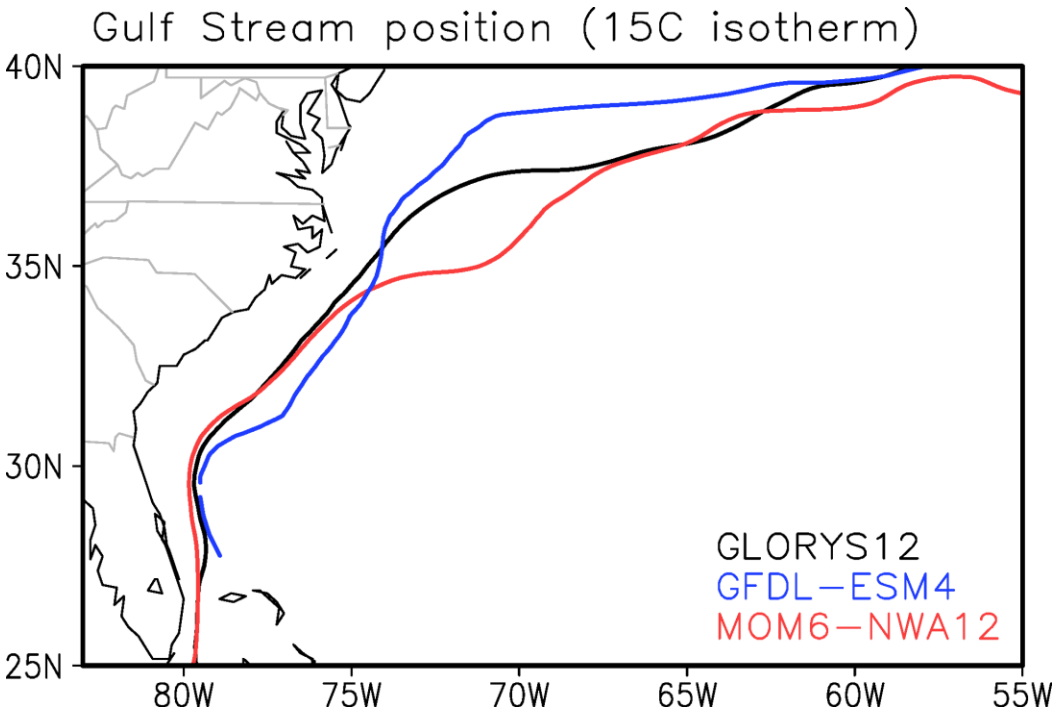

Fig. S1. The historical mean (1993-2020) position of the Gulf Stream (GS) in GLORYS12 (black line), GFDL-ESM4.1 (blue line), and MOM6-NWA12 (red line). The GS position is defined by the 15 °C isotherm at 200 m depth.

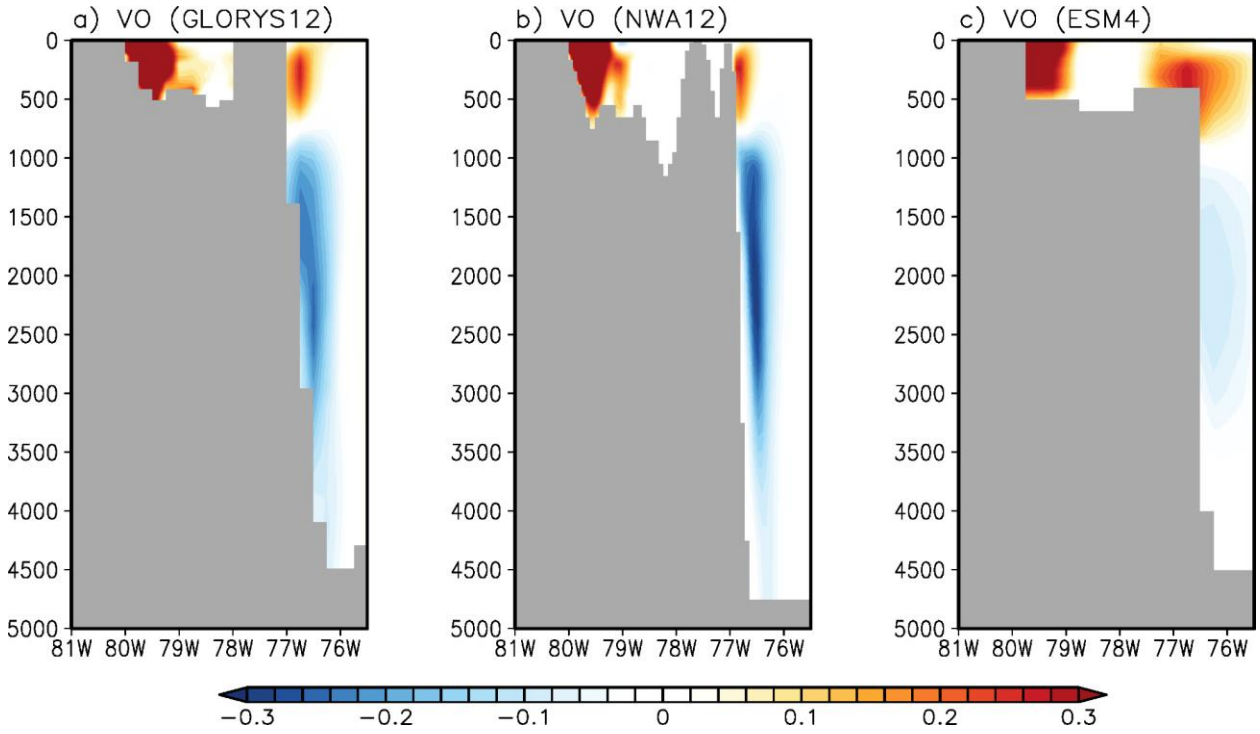

Fig. S2. The vertical cross section of meridional ocean speed at 26.5°N derived from (a) GLORYS12, (b) GFDL-ESM4.1 and (c) MOM6-NWA12

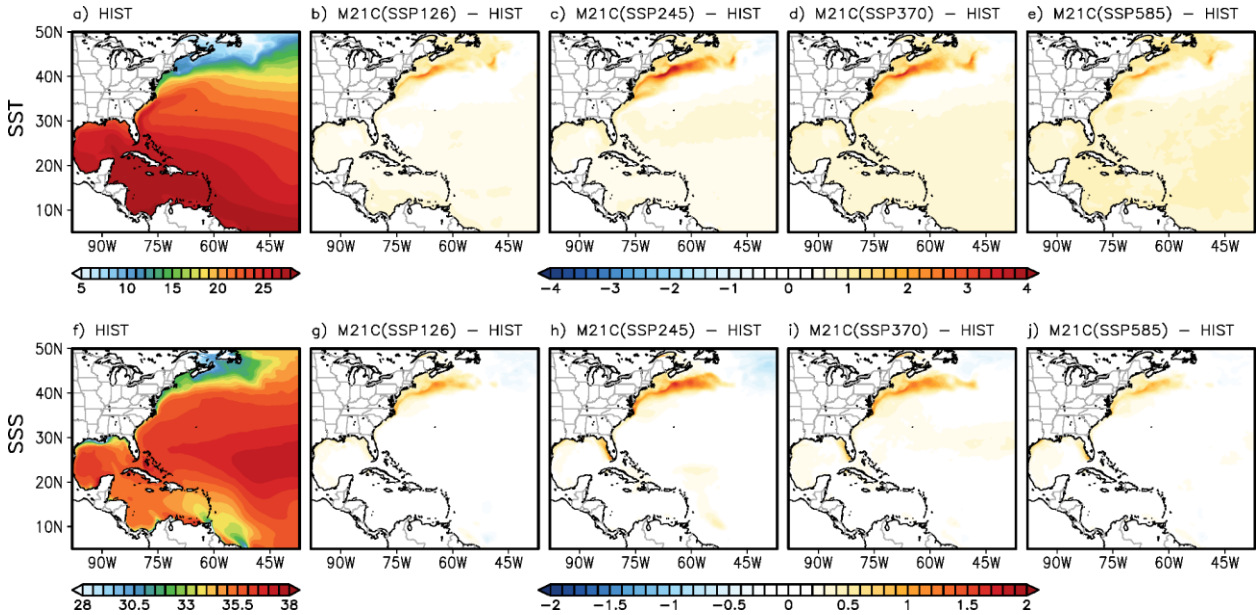

Fig.S3. (a) Spatial patterns of sea surface temperature (SST, °C) derived from MOM6-NWA12 during (a) historical period (1993-2020). The differences in SST between the mid 21st century (2025-2055) and historical periods in the (b) SSP-126, (c) SSP-245, (d) SSP-370 and (e) SSP-585 simulations. (f)-(j) are the same (a)-(e) but for sea surface salinity (SSS, psu).

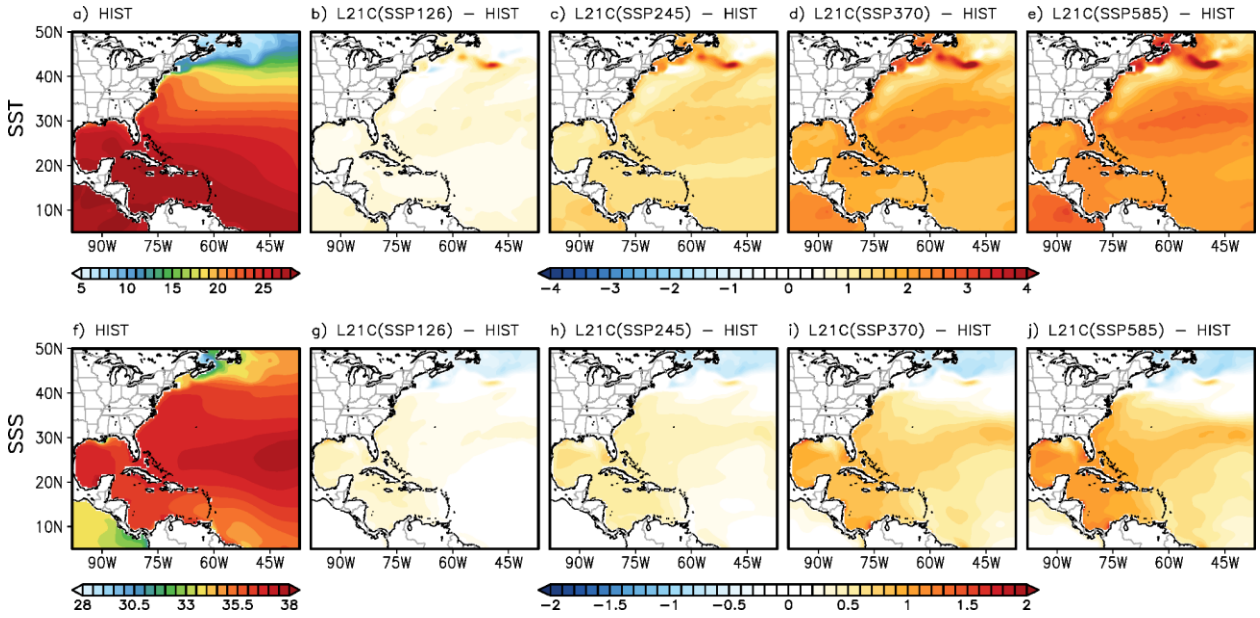

Fig.S4. (a) Spatial patterns of sea surface temperature (SST) derived from GFDL-ESM4.1 during the historical period (1993-2020). (b)-(e) are the differences in SST between the future (2073-2100) and historical (1993-2020) periods in the SSP-126, SSP-245, SSP-370, and SSP-585 simulations,respectively. (f) and (j) are the same (a) and (e) but for the sea surface salinity (SSS).

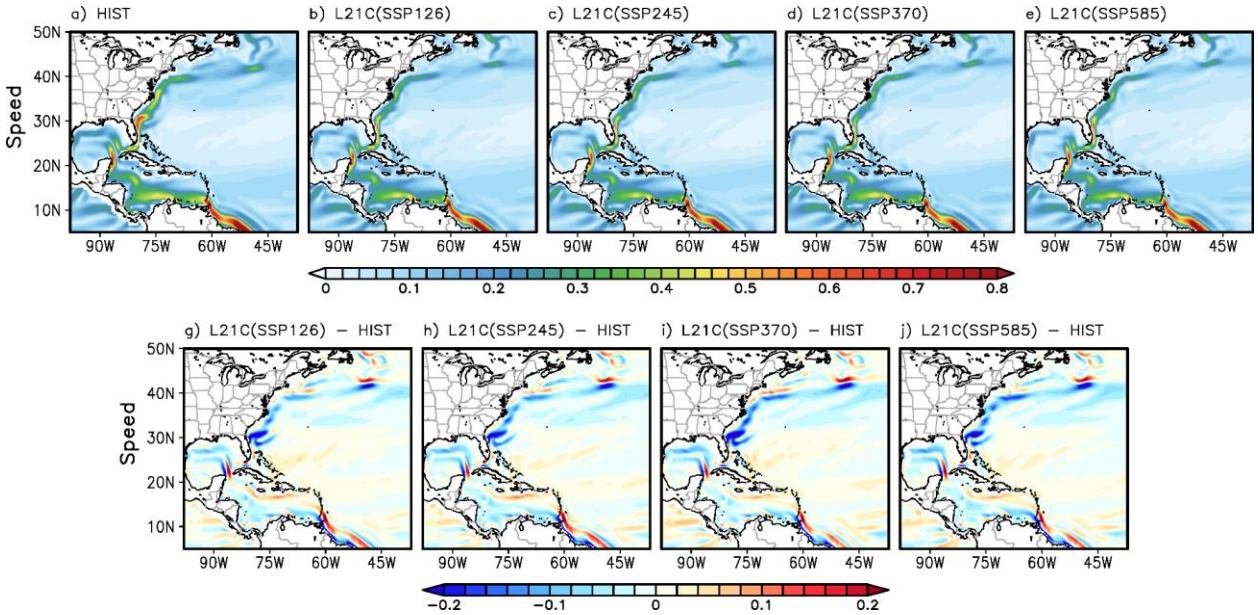

Fig. S5. Spatial surface current speed patterns derived from GFDL-ESM4.1 during (a) the historical (1993-2020) period, and future (2073-2100) period in the (b) SSP-126, (c) SSP-245, (d) SSP-370, and (e) SSP-585 simulations. The difference in surface current speed between the future and historical periods in (g) SSP-126, (h) SSP-245, (i) SSP-370, and (j) SSP-585 simulations, respectively.

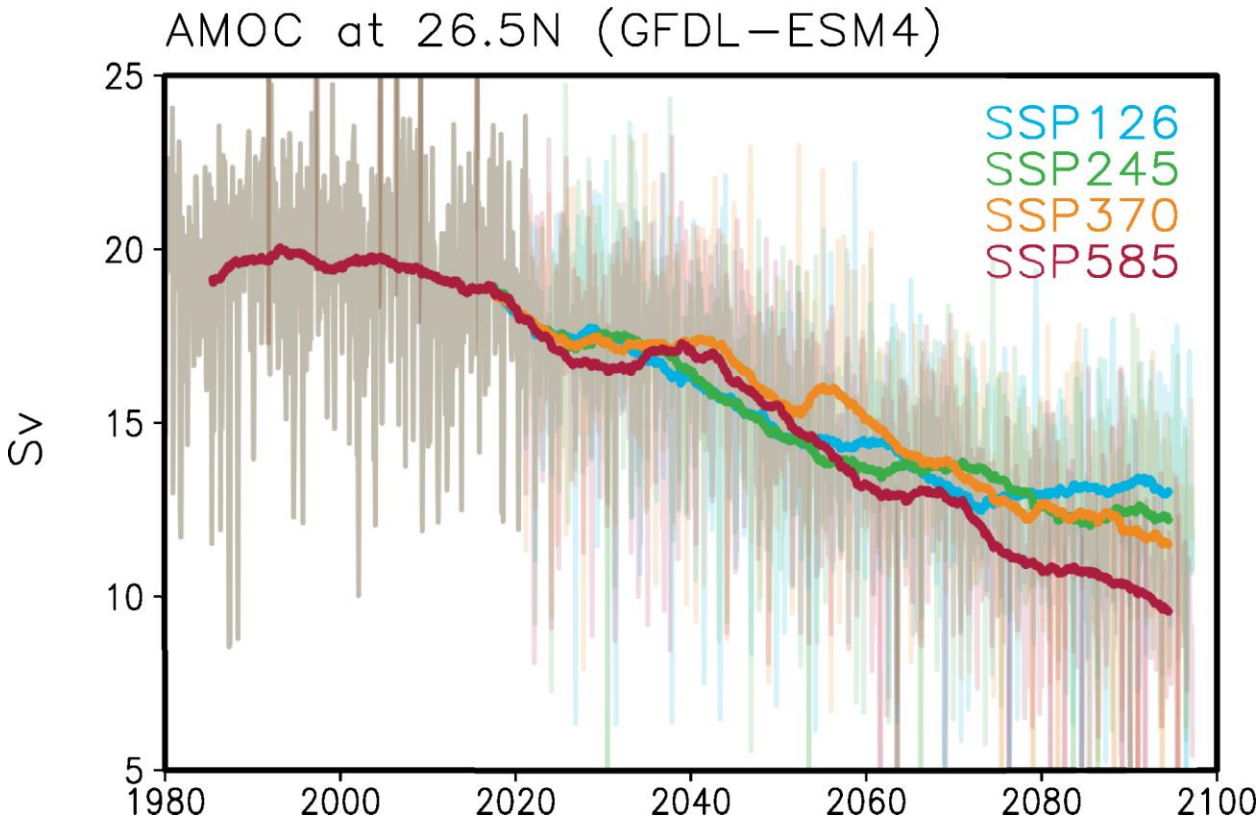

Fig. S6. Time series of AMOC in GFDL-ESM4.1. The blue, green, orange, and red lines are the SSP-126, SSP-245, SSP-370 and SSP-585 simulations, respectively.

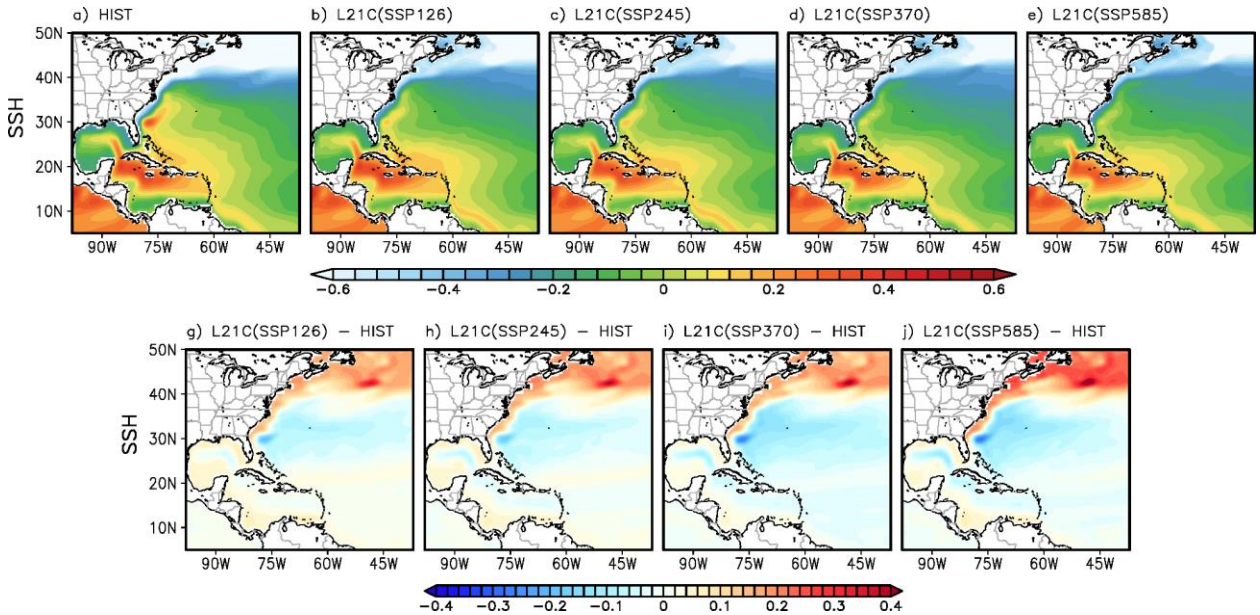

Fig S7. Spatial SSH patterns derived from GFDL-ESM4.1during (a) the historical (1993-2020) period, and future (2073-2100) period from (b) SSP-126, (c) SSP-245, (d) SSP-370, and (e) SSP-585 simulations, respectively. The difference in SSH between the future and historical periods from (g) SSP-126, (h) SSP-245, (i) SSP-370 and (j) SSP-585 simulations, respectively.